LPHYS2162 : INTRODUCTION TO THE PHYSICS OF THE CLIMATE SYSTEM AND ITS MODELLING

TEACHED BY F. RAGONE & H. GOOSE

Onto the study of multiple equilibria and abrupt changes of the oceanic thermohaline circulation

Mattias VAN EETVELT - 1660 18 00 & Max WIBERG - 1894 18 00

December 2023

1 Introduction

During this project we explore the model from Cessi (1994). This model describes in a rather simple manner the evolution of salinity and temperature in the ocean separating it in two water boxes in two different states that are subject to an external perturbation. Here that perturbation is a freshwater flux.

2 Model description

This simplified model has two boxes for two different latitudes of water with a respective temperature $T_1 = \theta/2$ and $T_2 = -\theta/2$, where $\theta/2$ is the relaxation temperature, a salinity S_1 and S_2. Each box interacts with the other box, through a transport term, $Q(\Delta\rho)$. In this model the external perturbation (forcing) of the salinity $F(t)$ is applied on one part of the box, and applied negatively on the other side, as shown by Fig. 1.

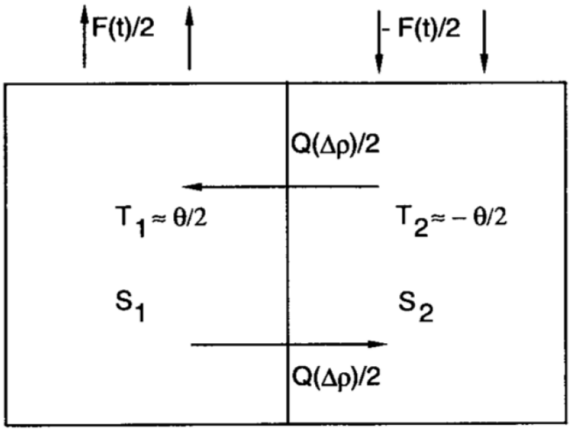

Figure 1: Schematic representation of the model, with two boxes of different salinity and temperature

The conservation equations for the temperature are:

$$\dot{T}_1 = -\tau_r^{-1}\left(T_1 - \frac{\theta}{2}\right) - \frac{1}{2}Q(\Delta\rho)(T_1 - T_2)$$
$$\dot{T}_2 = -\tau_r^{-1}\left(T_2 + \frac{\theta}{2}\right) - \frac{1}{2}Q(\Delta\rho)(T_2 - T_1)$$

where τ_r is the relaxation time for the temperature and θ is the relaxation temperature. The conservation equations for the salinity reads:

$$\dot{S}_1 = \frac{F(t)}{2H}S_0 - \frac{1}{2}Q(\Delta\rho)(S_1 - S_2)$$
$$\dot{S}_2 = -\frac{F(t)}{2H}S_0 - \frac{1}{2}Q(\Delta\rho)(S_2 - S_1)$$

$F(t)$ is the external salinity forcing which is represented as a freshwater flux, S_0 the reference state for the salinity and H is the depth of the ocean. Putting all these together and noting the difference in temperature and salinity as ΔT and ΔS, respectively. For the exchange function $\Delta Q(\Delta\rho)$ we use the definition proposed by Cessi (1994): $\Delta Q(\Delta\rho) = \frac{1}{\tau_d} + \frac{q}{V}(\Delta\rho)^2$ instead of the first one proposed by Stommel: $\Delta Q(\Delta\rho) = \frac{1}{\tau_d} + \frac{q}{V}|\Delta\rho|$, because it suits better the Boussinesq description of the exchange between the boxes due to convection. In this expression, τ_d is the diffusive timescale:

$$\begin{cases} \dfrac{d\Delta T}{dt} = -\dfrac{\Delta T - \theta}{\tau_r} - Q(\Delta\rho)\Delta T \\ \dfrac{d\Delta S}{dt} = \dfrac{F(t)}{H}S_0 - Q(\Delta\rho)\Delta S \\ Q(\Delta\rho) = \dfrac{1}{\tau_d} + \dfrac{q}{V}(\Delta\rho)^2 \end{cases}$$

Regarding the difference of density, we use the same definition of $\Delta\rho$ as the one proposed by Cessi (1994), $\Delta\rho = \alpha_S\Delta S - \alpha_T\Delta T$ with α being the linearization coefficients for the salinity and temperature.

An assumption that can be made is that when looking at the two timescales, that have order of magnitudes $\tau_r \approx 25$ days and $\tau_d \approx 220$ years, the temperature relaxation term is dominant in the first equation of the set here above. The temperature difference quickly becomes very close to the relaxation temperature, which allows us to assume $\Delta T = \theta$. The set of equation is reduced to a single equation since only the variation of salinity is considered:

$$\frac{d\Delta S}{dt} = \frac{F(t)}{H}S_0 - \frac{\Delta S}{\tau_d} - \frac{q}{V}(\alpha_S\Delta S - \alpha_T\theta)^2\Delta S \tag{1}$$

Values for the different terms in this equation are listed in appendix A.

3 Results

3.1 Deterministic process

With all the values fixed as presented in appendix A, a constant value of $F(t) = \bar{F} = 3.24$ m.years^{-1}, and assuming that left term of (1) is null, i.e.

$$\frac{d\Delta S}{dt} = 0 \quad \Leftrightarrow \quad 0 = \frac{\bar{F}}{H} S_0 - \frac{\Delta S}{\tau_d} - \frac{q}{V}(\alpha_S \Delta S - \alpha_T \theta)^2 \Delta S \tag{2}$$

Eq. 2 is solved for a range of values of ΔS. The solution and the corresponding potential are computed (Fig. 2).

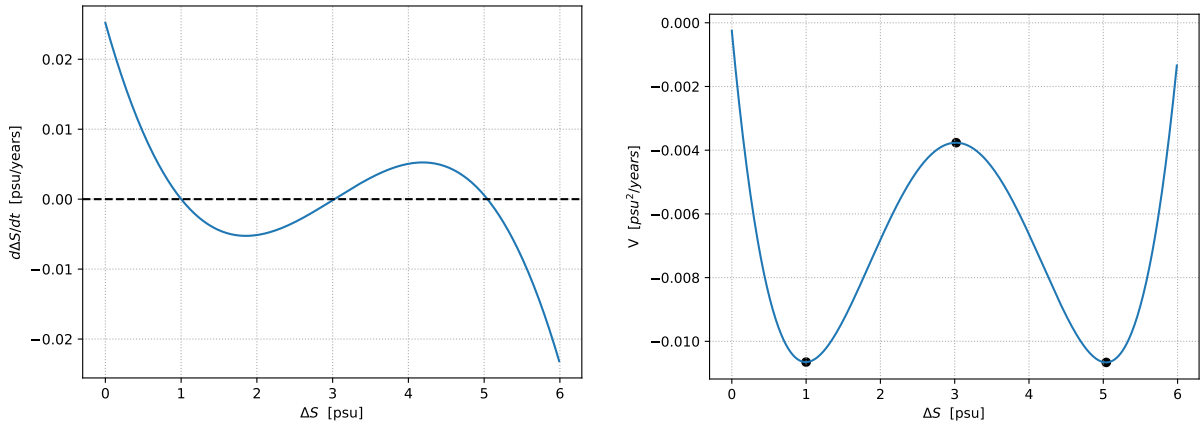

(a) (b)

Figure 2: (a) $d\Delta S/dt$ evolution for $\bar{F} = 3.24$ m.years^{-1} and (b) the corresponding potential. Extremas are located at values of $\Delta S = 1,\ 3.02$ and 5.04 psu

Cessi (1994) proposes $\bar{F} = 2.3$ m.years^{-1} as an representative estimation of the fresh water flux. For the latter value, the system has only one stable solution. However, for $\bar{F} = 3.24$ m.years^{-1} the same system displays two stable solutions. Thus the critical value of $\bar{F}$ for which the number of stable solutions changes lies between these bounds. The critical value is first graphically estimated (Fig. 3). The graphical interpretation suggests that this value is comprised between $\bar{F} = 2.5$ m.years^{-1} and $\bar{F} = 2.6$ m.years^{-1}.

Subsequently, the critical value is numerically estimated by counting the number of times that the solution changes sign (i.e. the number of time the solution crosses the line $x = 0$). The resulting critical value is $\bar{F} = \bar{F}_c = 2.5649$ m.years^{-1}. This value corresponds to the first value of $\bar{F}$ for which the solution admits more than one stable solution, with an accuracy of 0.001 m.years^{-1} (Fig. 4)

Finally, eq. 1 is integrated using a Forward-Euler scheme, for three values of $\bar{F}$: under, over and at the critical value, and for various initial conditions (Fig. 5).

3.2 Stochastic process

In the second part of this work, the freshwater flux was considered to be composed of a deterministic part $\bar{F}$ and a stochastic part $F'(t)$ such that $F(t) = \bar{F} + F'(t)$. This yields the following equation:

$$\frac{d\Delta S}{dt} = \frac{\bar{F} + F'(t)}{H} S_0 - \frac{\Delta S}{\tau_d} - \frac{q}{V}(\alpha_S \Delta S - \alpha_T \theta)^2 \Delta S \tag{3}$$

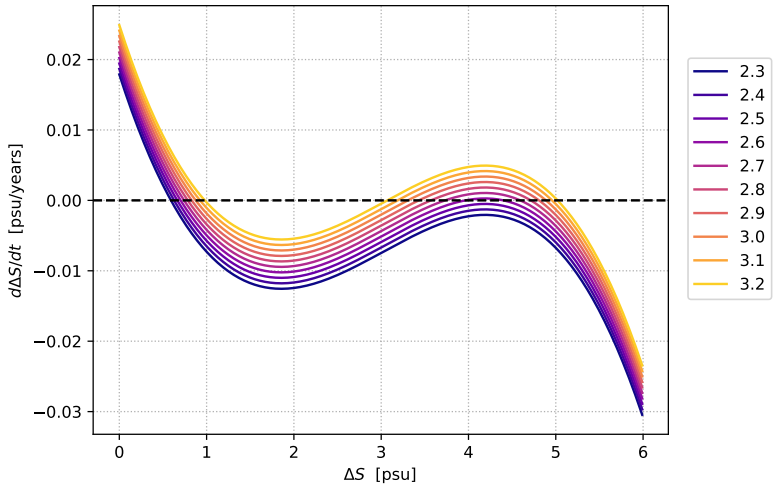

Figure 3: Graphical estimation of the critical value $\bar{F}_c$, using values of $\bar{F}$ ranging from 2.3 to 3.2 m.years^{-1}

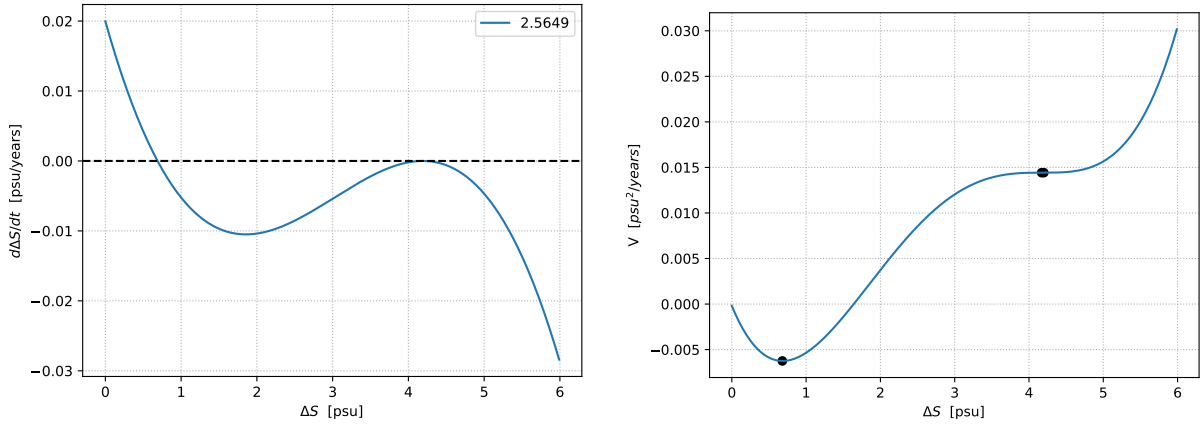

(a) (b)

Figure 4: (a) $d\Delta S/dt$ evolution for $\bar{F} = \bar{F}_c = 2.5649$ m.years^{-1} and (b) the corresponding potential. Extremas are located at values of $\Delta S = 0.68,\ 4.17$ and 4.2 psu

Equation 3 is integrated using a Forward-Euler scheme with an initial condition of $\Delta S = 3$ psu (Fig. 6).

4 Discussion

For a purely deterministic process and a constant value of $F(t) = \bar{F} = 3.24$ m.years^{-1}, the studied system is bistable. There are two stable solutions at 1 and 5.04 psu, respectively. The former solution corresponds to a substantial transport state whereas the latter corresponds to a weak one. The third solution at 3.02 psu is linearly unstable, as illustrated in Fig. 2b. Starting at the latter solution, the system will easily "roll off" into either one of the two wells, corresponding to the two stable solutions. Additionally, as the wells are rather deep for this value of $\bar{F}$, it suggests that an important perturbation is needed to switch from one solution to the other.

For lower values of net freshwater flux, however, only one stable stable solution exists, as it is shown on Fig. 3. The critical value $\bar{F}_c$ is the first value for which the system showcases two

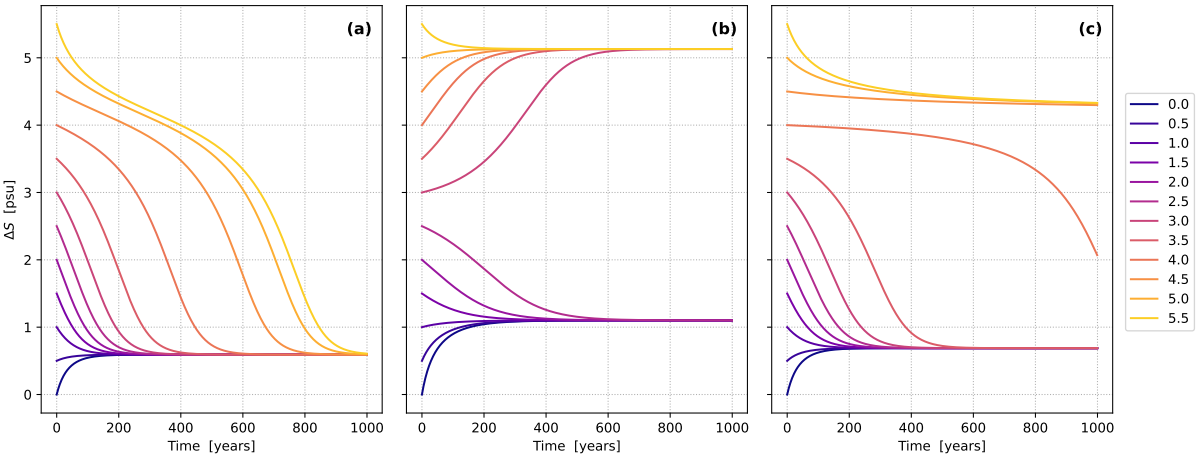

Figure 5: Time series solution of eq. 1 for various values of $\bar{F}$: (a) 2.3 m.years^{-1}, (b) 3.4 m.years^{-1}, and (c) 2.5649 m.years^{-1}. The various lines in each plot correspond to various initial conditions of ΔS [psu]

stable solutions. The potential for $F(t) = \bar{F}_c$ shows that there are indeed two stable solutions, though the second solution is hard to observe as the corresponding well's depth is small. (Fig. 4b). A system at around 4 psu can either converge towards the first (0.68 psu) or the second (4.2 psu) solution, but the first solution seems more stable than the second one. Besides, the rate at which the system will converge towards one solution is greater for $\bar{F} = 3.24$ m.years^{-1} than for $\bar{F}_c = 2.5649$ m.years^{-1}, as the respective potential's slopes are steeper for the former case.

These various converging rates can be observed on Fig. 5. The first two subfigures, (a) and (b), respectively show the case where the system has one and two stable solutions. In the former scenario, the rate at which the system converges towards the solution only depends on how far the initial condition is from the single solution. The relaxation time thus ranges from, roughly, 150 years when the initial condition is close to the solution, to 1000 years in the opposite case. For the latter scenario, the system will converge to one solution depending on which side of the double-well-shaped potential lies the initial condition. The relaxation time ranges from 150 years to 600 years, which is significantly shorter than the first scenario. Finally the last subfigure, (c), which corresponds to a critical freshwater flux forcing, shows that the convergence rate for the second solution (4.2 psu) is lesser than for a more important forcing, such as $\bar{F} = 3.4$ m.years^{-1}. This is explained by the almost flat potential around 4 psu (Fig. 4b). Therefore, the system won't easily "roll off" towards the solution at 4.2 psu. This is clearly noticeable for an initial condition of 4 psu : after 1000 years, the system still hasn't converged to the first solution (0.68 psu).

In the second part of this work, we considered a stochastic forcing. Fig. 6 shows a typical time series solution. With a stochastic forcing of the order of $\sigma = 3\bar{F}$, the system clearly oscillates between both deterministic solutions. However, with these parameters, the system needs approximately 20,000 years for a transitions to happen. The distribution of the time spent by the system at the two solution seems even. Computing the ensemble (N=100) histogram shows that the second solution is slightly dominant, for the given parameters (Fig. 7). This almost-even distribution was expected as the respective potential appears to be symmetric and showcase two deep wells.

Intuitively, it is expected that the system will struggle to jump between both deterministic solutions if the stochastic forcing is weaker, while keeping the same deterministic forcing (i.e.

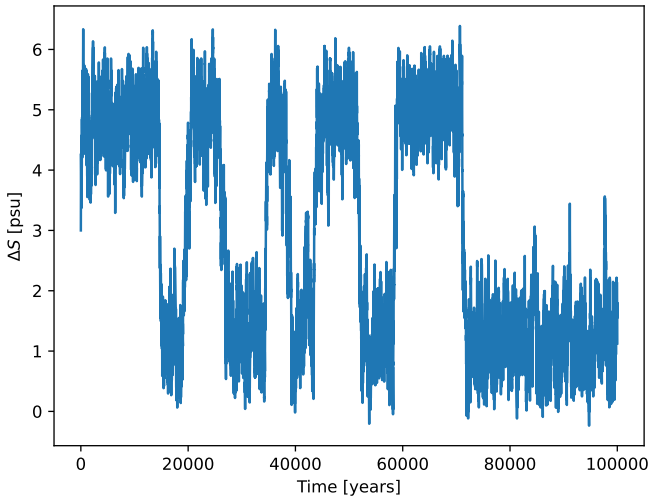

Figure 6: Stochastic time series solution of eq. 3 At every time step, the stochastic forcing is randomly picked from a Gaussian distribution with zero mean and standard deviation of $\sigma = 3\bar{F}$ and $\bar{F} = 3.25$ m.years^{-1}

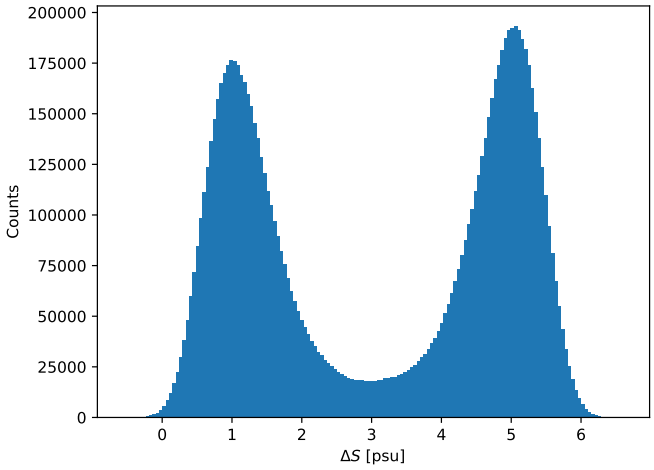

Figure 7: Histogram of the ensemble for 100 realizations. All the parameters are the same as in Fig. 6

$\bar{F} = 3.25$ m.years^{-1}). This behaviour is noticeable on Fig. 8 : for weaker values of stochastic forcing, the system tends to jump less between the two deterministic solutions. Additionally, when the forcing is sufficiently weak, the system ceases to jump altogether. Graphically, this results in thinner distributions as the amplitude of the noise is smaller for weaker forcing values. Another consequence is that there are less values outside of the range of the solutions (e.g. around 3 psu). This simply results from the fact that the system never reaches these values, because the stochastic forcing is not strong enough to do so.

Subsequently, various values of $\bar{F}$ are tested to try to showcase the properties of the time evolution of the system in different conditions (Fig. 9). For increasing values of $\bar{F}$, the system inevitably switches from one solution to two solutions. When a stochastic forcing is applied, this results in an increase of jumps between the two deterministic solutions. Indeed, as the freshwater flux is increased, so does the magnitude of the noise since $\sigma = 3\bar{F}$, as well as the slopes of the corresponding potential (i.e. the well's depth), as discussed previously. Thus the resulting system has both the characteristics and the ability to jump between both solutions.

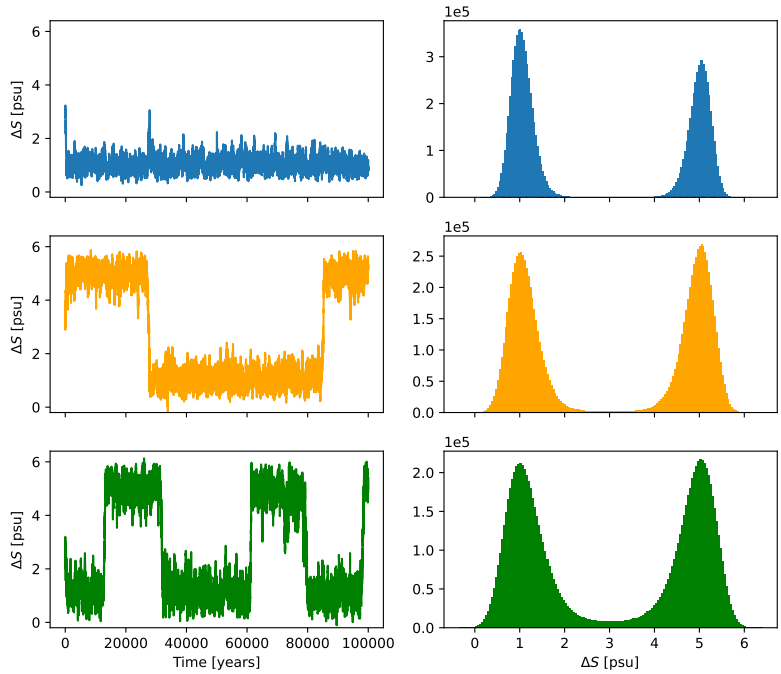

Figure 8: Typical time series solutions and ensemble histograms (100 realizations) for various stochastic forcing values : $\sigma = 1.5\bar{F}$: blue, $\sigma = 2\bar{F}$: orange and $\sigma = 2.5\bar{F}$: green. The noise is sampled as in Fig. 6

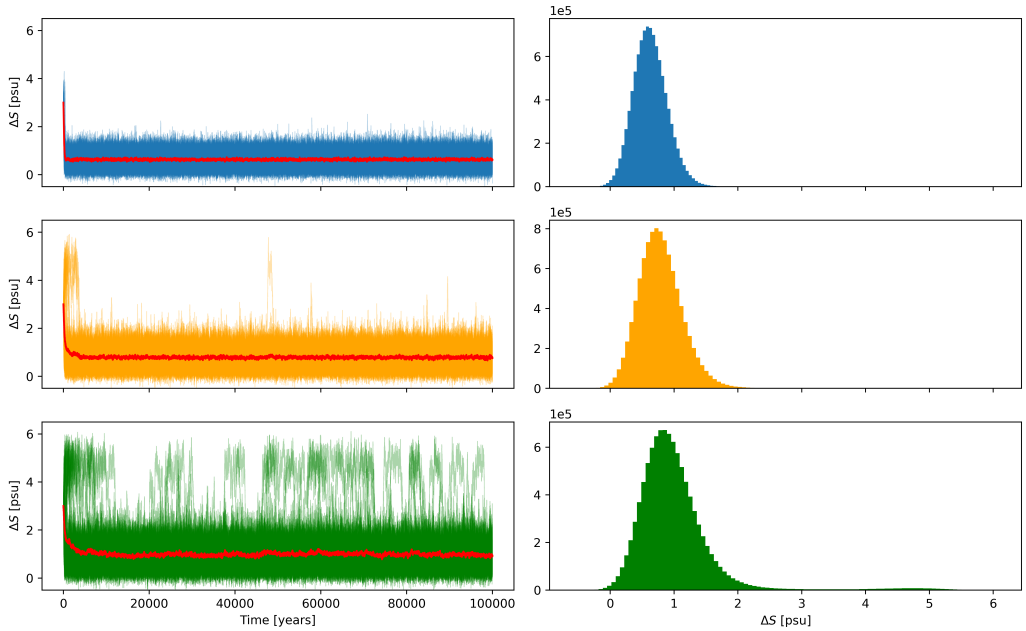

Figure 9: All time series solutions of the ensemble (100 realizations) with the ensemble mean (red line) for various values of $\bar{F}$ and the corresponding ensemble histogram. Blue : $\bar{F} = 2.3$ m.years^{-1}, orange : $\bar{F} = 2.65$ m.years^{-1} and green : $\bar{F} = 2.9$ m.years^{-1}. The noise is sampled as in Fig. 6

Furthermore, this behaviour transition is also observable on the respective histograms. The distribution are wider for greater values of freshwater flux, with more values clustering around the second solution at approximately 5 psu.

5 Conclusion

The simple two-box model proposed by Cessi (1994), representing the ocean circulation, was studied.

In section 3.1 we showed that depending on the freshwater flux forcing, the system has one or two stable equilibria. Practically, this means that the Atlantic Meridional Overturning Circulation (AMOC) could switch from a substantial transport state towards a weak one. Additionally, we showed that depending on the considered equilibrium, the relaxation time is significantly longer when the system only admits one solution.

In section 3.2, we considered the forcing to be composed of both a deterministic and stochastic part. For a strong enough deterministic forcing causing multistability, this lead to fluctuations around both equilibria as well as jumps between both states. We then tested various stochastic forcing values. This resulted is lesser jumps between equilibria, confirming the intuitive idea that a strong enough fluctuation is needed to overcome the potential barrier. Indeed, the ability of the system to jump between solutions depends on the variance of the stochastic forcing. Finally, various values of $\bar{F}$ are tested to showcase the properties of the system's time evolution in different conditions. For increasing freshwater flux values, we showed that the resulting systems have both the required multistability and strong enough forcing to transition from one solution to the other.

Altogether, this supports that the AMOC collapse represents a realistic future.

6 References

Cessi, P. (1994). A simple box model of stochastically forced thermohaline flow. *Journal of Physical Oceanography*, 24(9):1911–1920.

A Parameter values

Table 1: All parameter values for equation 1 and 3

Parameter	**Value**	**Unit**
V	1.1137×10^{16}	m^3
L	8250×10^3	m
H	4500	m
σ_w	300×10^3	m
τ_d	219	$years$
θ	20	$^\circ C$
S_0	35	psu
α_T	0.17×10^{-3}	$^\circ C^{-1}$
α_S	0.75×10^{-3}	psu^{-1}
q	3.27×10^{19}	$m^3.years^-1$
F	*varies*	$m.years^{-1}$